Synthesis and Characterization of Nanosized Nickel substituted Cobalt-Zinc Ferrite

Nway Nway Khaing[1], Phyu Phyu Khaing[1], Hla Htay[1], Win Kyaw[1], Win Win Thar[2] and Khin Mar Kyu[1]

[1]*Department of Physics, University of Yangon, Myanmar*
[2]*Department of Physics, Dagon University, Myanmar*

Abstract. Nanosized Nickel substituted Cobalt-Zinc ferrites with the formula $Co_{0.5-x}Ni_xZn_{0.5}Fe_2O_4$ (where x = 0, 0.1, 0.2, 0.3) were chosen and prepared by co-precipitation method by decomposition of their respective metal chlorides and zinc sulphate heptahydrate. The heat treatment of the ground precursor powders at their respective decomposition temperature and beyond, results in the evolution of heat from the combustion of the residual chlorides and sulphate materials. This facilitates the reactions among the constituent metal ions and the formation of the desired oxide phase at low temperature. The average crystallite sizes were determined from X-ray pattern. The FTIR studies have been used to confirm the formation of metal oxide. The migration of Fe^{3+} ion from octahedral site to tetrahedral site decreases the electrical conductivity with increase in nickel concentration due to the charge libration and electron hoping together form the basis for the conduction mechanism.

Keyword: Nanosized ferrites, decomposition, X-ray diffraction, FTIR, electrical conductivity
PACS: 68

INTRODUCTION

Ferrite materials are insulating magnetic oxides [1]. Spinel ferrites are extremely important for academic and technological applications [2]. Spinel ferrites have been studied extensively due to their low prices, easy to fabricate and abundant uses in technological and industrial applications [3]. The useful properties of the spinel ferrites mostly depend upon the chemical composition, preparation methods, sintering temperature, nature of the additives and their distribution i.e. tendency to occupy tetrahedral (A) or octahedral (B) site.

There has been renewed interest in fine magnetic particles with the possibilities of applications in the field of nanostructured materials technology opening up in the last few years. The interest in the wet-chemical synthesis of ultrafine ferrite powders enabling production of ceramics with high density at low temperatures is unquestionable. In many commercial applications, like transformer cores, chokes, high density recording media, microwave devices etc., the dc resistivity of the spinel ferrites play a vital role which can be controlled by selecting a suitable sintering scheme and/or by addition of small amount of suitable element [4]. The ferrites having high dc resistivity and low coercivity are very useful in making switching devices [5, 6].

Many studies on Co-Zn ferrites in the bulk crystalline form were prepared by usual ceramic technique [7]. Ram Kripal Sharma et al. (2005) has reported the synthesis of chromium substituted nano particles of cobalt zinc ferrites by co-precipitation method [8]. Sonal Signaj et al. (2005) has reported preparation and characterization of nano sized nickel substituted cobalt ferrite [9]. Gul et al. (2007) has prepared nanoparticles of $Co_{1-x}Zn_xFe_2O_4$ with stoichiometric proportion (x) varying from 0.0 to 0.6 by the chemical co-precipitation method [10]. Praveena et al. (2013) has reported the elastic behavior of Sn doped Ni-Zn ferrites [11]. In this paper, the effects of small addition of Ni on the structural, vibrational and electrical properties of Cobalt-Zinc ferrites ($Co_{0.5-x}Ni_xZn_{0.5}Fe_2O_4$) have been reported.

MATERIALS AND METHODS

The co-precipitation technique has been used to prepare the nanosized $Co_{0.5-x}Ni_xZn_{0.5}Fe_2O_4$. Aqueous solutions of Analar (AR) grade $NiCl_2.6H_2O$, $ZnSO_4.7H_2O$, $CoCl_2.6H_2O$ and $FeCl_3$ with desired stoichiometric compositions were mixed thoroughly stirrer at 80°C using magnetic-stirrer. Then it was transferred immediately into a boiling solution of NaOH under stirring throughout the reaction. Conversion of metal salts into hydroxides and subsequent transformation of metal hydroxide into ferrites took place upon 100°C and maintained for 1 h until the reaction was complete. The ferrites thus formed were isolated by centrifugation and washed several times with deionized (DI) water followed by acetone and then dried at room temperature. The dried ferrites powders were ground by ball-milling and for further heat treatment and structural characterizations.

Thermal decompositions were investigated by simultaneous thermogravimetric and differential thermal analysis (TG-DTA) using a SHIMADZU DTG-60H instrument. Then ferrites powders were annealed at 600°C for 2 h using laboratory-built furnace.

X-ray powder diffraction patterns were recorded on a RIGAKU MULTIFLEX, X-ray Powder diffractometer

using CuK_α radiation (λ = 1.54056 Å) in 2θ range 10°–45°. The crystallite size was calculated by Scherrer's formula, using the full width at half maximum intensity for (311) plane of the pattern.

The Fourier transform infrared spectra were recorded using infrared spectrometer (SHIMADZU, FTIR-8400) in the range 400–2000 cm^{-1} for precursors and for as-prepared samples of x = 0, 0.1 and 400–4000 cm^{-1} for as-prepared samples of x = 0.2, 0.3. The samples were prepared in the form of pellets in the KBr medium.

For measuring the electrical properties, the samples were made pellets with the same in diameters 1.306 cm and thicknesses 0.473 cm, 0.601 cm, 0.474 cm, 0.573 cm for x = 0, 0.1, 0.2, 0.3 respectively. The temperature dependent dc resistivity was measured by using two probe method in the temperature range of 299 K – 773 K. Silver paste electrodes were formed on both the sides of the pellets and electrical connections were formed with the copper wire leads. The samples were inserted between two electrodes inside a cell supported by a furnace. The electrical resistances were observed by using FLUKE 45 Dual Display Multimeter.

RESULTS AND DISCUSSION

Thermal Analysis of Coordination Compound

Simultaneous thermogravimetric and differential thermal analysis (TG-DTA) of the precipitated ferrite precursors were carried out with a heating rate 20°C min^{-1} in N_2 atmosphere. Fig. 1(a) and (b) show the TG-DTA thermograms of the ferrite precursors of $Co_{0.5}Zn_{0.5}Fe_2O_4$ (x = 0) and $Co_{0.2}Ni_{0.3}Zn_{0.5}Fe_2O_4$ (x = 0.3).

The decomposition temperatures were found to lie between 35°C and 600°C in TG thermogram of x = 0 with the mass variation of 29.08%. A deep endothermic trough around 90°C is attributed to the decomposition of chlorides and sulphate in DTA thermogram. A broad endothermic reaction peak around 235°C is indicated by the dehydration from the starting materials. An exothermic reaction peak in DTA is found at 326°C and beyond that indicated by the combustion reaction was completed.

The TG-DTA thermograms of x = 0.3 ferrite precursor is shown in Figure 1(b). The TG thermogram was found to the same in pattern with x = 0 with the mass variation of 35.73%. A large endothermic peak with step-wise reaction is found at 110°C and an exothermic reaction peak is clearly found at 396°C in DTA thermogram. The thermal decomposition processes are the same as the $Co_{0.5}Zn_{0.5}Fe_2O_4$ thermograms. The decomposition and dehydration temperatures were found to shift due to the influence of Nickel substituted in Cobalt-Zinc ferrite. The desired phase formation temperature of the precipitated ferrite precursors is well determined from the results of thermal analysis and it is obtained as around 600°C.

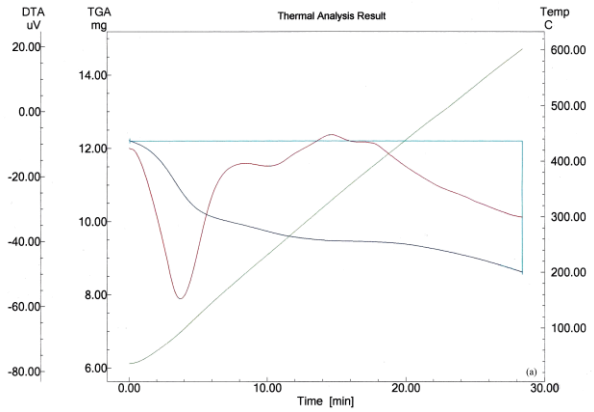

FIGURE 1.(a) TG-DTA thermograms of $Co_{0.5}Zn_{0.5}Fe_2O_4$ ferrite precursor

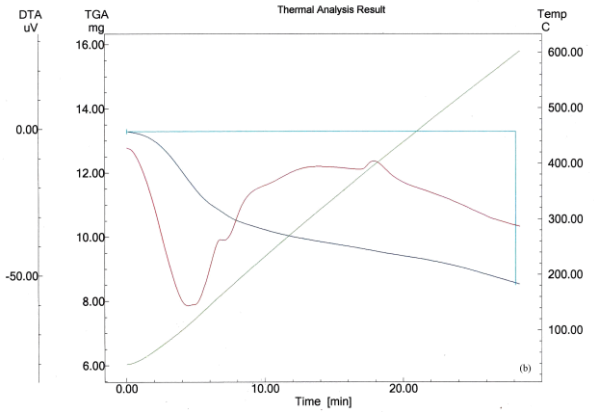

FIGURE 1.(b) TG-DTA thermograms of $Co_{0.2}Ni_{0.3}Zn_{0.5}Fe_2O_4$ ferrite precursor

X-Ray Diffraction Analysis

X-ray diffraction (XRD) patterns of the as prepared samples are shown in Fig. 2. The sharp lines and absence of impurity peaks in the X-ray diffraction pattern indicates the formation of crystalline single-phase spinel structure. All the peaks appeared in XRD can be identified with the spinel $ZnFe_2O_4$, $CoFe_2O_4$, $NiFe_2O_4$ and no impurity peaks of either ZnO, CoO, NiO, or Fe_2O_3 confirms the proper phase formation of $Co_{0.5-x}Ni_xZn_{0.5}Fe_2O_4$ at temperature 600°C.

The XRD studies reveal that nanosized of spinel ferrites formed by chemical co-precipitation method are crystalline. The lattice parameters "*a*" for the different Nickel concentrations were calculated using the equation;

$$a = \frac{\lambda}{2\sin\theta}\sqrt{h^2+k^2+l^2}\ .$$

Crystallite sizes below roughly 100 nm can be accurately evaluated using powder diffraction technique. The fine particle nature of the ferrite is reflected in the X-ray line broadening. The values of crystallite size "*D*" were calculated from the most intense lines (I = 100%) of (311) planes in the collected XRD patterns for the different Nickel concentrations, using Scherrer's equation;

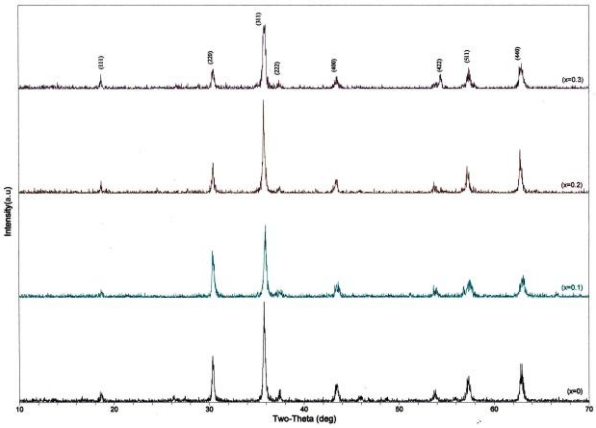

FIGURE 2. X-ray powder diffraction patterns of the $Co_{0.5-x}Ni_xZn_{0.5}Fe_2O_4$ ferrites

$$D = \frac{0.9\lambda}{\beta \cos\theta}$$

where, λ is the wavelength of X-ray, β is the full width at half maxima (FWHM) and θ is the Bragg angle. Variations of the lattice parameters and the crystallite size with different Nickel concentrations are shown in Fig. 3(a) and (b). The experimental results are tabulated in Table 1.

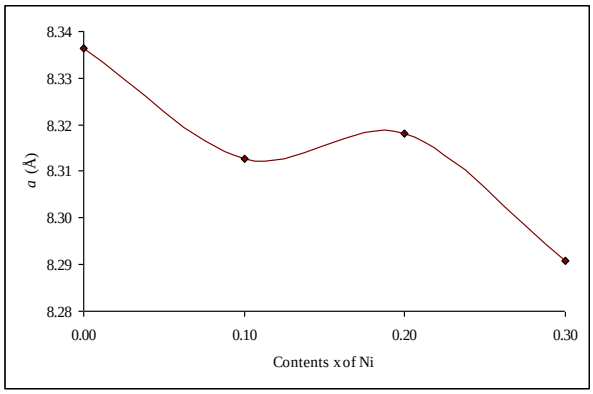

FIGURE 3.(a) Variation of the lattice parameters with different Nickel concentration in $Co_{0.5-x}Ni_xZn_{0.5}Fe_2O_4$ ferrites

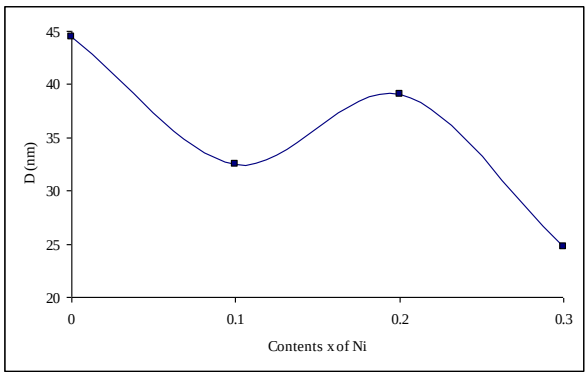

FIGURE 3.(b) Variation of the crystallite sizes with different Nickel concentration in $Co_{0.5-x}Ni_xZn_{0.5}Fe_2O_4$ ferrites

As shown in Fig. 3(a), the lattice parameters of the $Co_{0.5-x}Ni_xZn_{0.5}Fe_2O_4$ ferrites are found alternately due to The cations distribution of $(Co_{1-x}Zn_{0.5}Fe)[Ni_xFe]O_4$ where the brackets ( ) and [ ] denote A-site and B-site, respectively. Such cation distribution is based on the following facts:

(1) Ni^{2+} ions have a strong preference to occupy the B-site while Co^{2+} and Zn^{2+} ions have a strong preference to occupy the A-site.

(2) As for Ni-ion distribution, it is reported that Ni^{2+} ions strongly prefer to occupy the A-site for low Ni-concentration. However, for high Ni-concentration, it is suggested that the Ni^{2+} ions are either distributed between A-site and B-site or reside at the grain boundaries. Thus, according to the assumed cation distribution, increasing of the Ni-concentration from x = 0.1 to x = 0.3 leads Fe^{3+} content in B-site to decrease and that in A-site to increase.

As shown in Figure 3(b), the crystallite sites of the $Co_{0.5-x}Ni_xZn_{0.5}Fe_2O_4$ ferrites are also found alternately with increasing contents x of Ni. The crystallite site of undoped Co-Zn ferrite is obtained as 44.42 nm and the Ni (x = 0.3) doped Co-Zn ferrite is obtained as 24.79 nm.

TABLE 1. Variation of the lattice parameters and crystallite sizes of $Co_{0.5-x}Ni_xZn_{0.5}Fe_2O_4$ ferrites

x	β (°)	a (Å)	D (nm)
0	0.188	8.3363	44.42
0.1	0.241	8.3128	32.46
0.2	0.214	8.3181	39.08
0.3	0.337	8.2908	24.79

FTIR Analysis

Fourier transform infrared (FTIR) spectroscopy is an excellent analytical tool to study the distribution of the cations in the tetrahedral and octahedral sites in ferrite system. The IR absorption band changes with the change introduced in the A-site and B-site cation distributions in the ferrite system. It is also used to determine the local symmetry in crystalline solids, ordering phenomenon in spinels and presence/absence of Fe^{2+} ions.

FTIR transmission spectra of $Co_{0.5-x}Ni_xZn_{0.5}Fe_2O_4$ (where x = 0, and 0.3) are shown in Fig. 4(a) and (b) for precursors and Fig. 5(a) and (b) for as-prepared samples. In the normal spinel ferrite, there are four fundamental modes (ν_1, ν_2, ν_3 and ν_4) of infrared (IR) lattice vibrations. Normally, two absorption bands below the wavenumber 650 cm^{-1} is a common feature of all the ferrites. The lines are sometimes splitting due to the conditions of crystalline environments. Table 2(a) and (b) show the details assignments of precursors and Table 3(a) and (b) show the as-prepared samples.

The bands arise from the lattice vibrations of the oxide ions against the cations. Intrinsic stretching vibrations of the metal at the tetrahedral site, $M_{tetra} \leftrightarrow O$, assigned as ν_1, are generally observed in the range of 620-550 cm^{-1}. Octahedral-metal stretching

vibrations, $M_{octa} \leftrightarrow O$, ν_2-lowest band, are generally observed in the range of 450-385 cm^{-1} [12, 13].

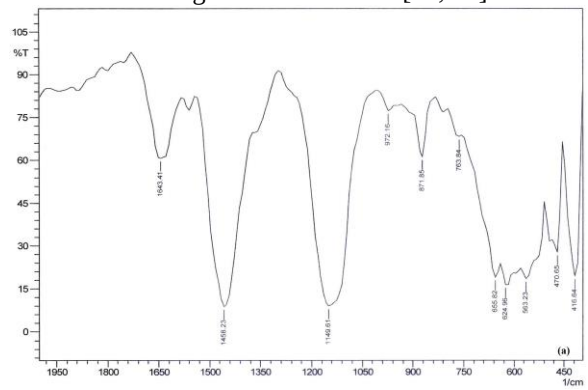

FIGURE 4.(a) FTIR transmission spectrum of $Co_{0.5}Zn_{0.5}Fe_2O_4$ ferrite precursor

In Fig. 4(a) and (b), ν_1 stretching vibration of as-prepared ferrites was observed at 563 cm^{-1}, 625 cm^{-1} and 656 cm^{-1} for x = 0 and 525 cm^{-1} and 594 cm^{-1} for x = 0.3. The ν_2 stretching vibration was observed at 417 cm^{-1} and 471 cm^{-1} for x = 0 and 417 cm^{-1} and 478 cm^{-1} for x = 0.3. It was found that a shift in wavenumber indicates the Nickel concentration on Co-Zn ferrite. The lines at 763 cm^{-1} and 872 cm^{-1} in x = 0 and 872 cm^{-1} in x = 0.3 were attributed by the stretching band of Co-Zn-O-Fe bond of the tetrahedral building forming the structure. Vibrational peaks of starting materials were not found in Fig. 5(a) and (b), and it indicated that the ferrite formation from XRD

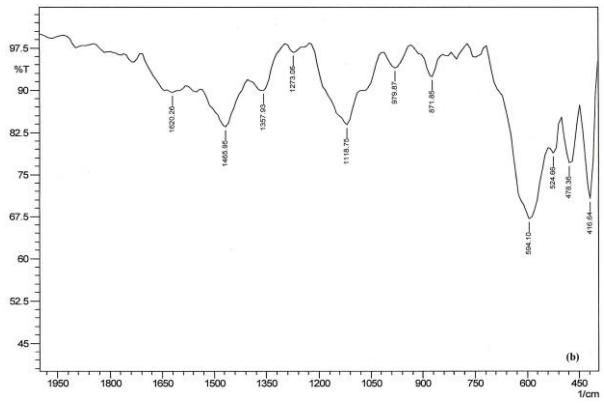

FIGURE 4.(b) FTIR transmission spectrum of $Co_{0.2}Ni_{0.3}Zn_{0.5}Fe_2O_4$ ferrite precursor

TABLE 2.(a) Wavenumbers and corresponding vibrational modes assignments of ferrite precursor for x = 0

Wavenumber (cm^{-1})		Mode assignment	Molecular Group
Observed	Standard		
417/471	450	ν_2-mode	Co^{2+}-Zn^{2+} in T_d-site
563/625/ 656	550	ν_1-mode	Fe^{3+} in O_h-site
763/872	825	Stretching	Co-Zn-O-Fe
972	981	ν_1-mode	SO_4^{2-}-stretching
1150	1125	ν_3-mode	SO_4^{2-}-dipole
1458	1440	Stretching	-OH
1643	1638	ν_2-mode	H_2O-bending

TABLE 2.(b) Wavenumbers and corresponding vibrational modes assignments of ferrite precursor for x = 0.3

Wavenumber (cm^{-1})		Mode assignment	Molecular Group
Observed	Standard		
417/478	450	ν_2-mode	Ni^{2+}-Co^{2+}-Zn^{2+} in T_d-site
525/594	550	ν_1-mode	Fe^{3+} in O_h-site
872	825	Stretching	Co-Ni-Zn-O-Fe
980	981	ν_1-mode	SO_4^{2-}-stretching
1119/ 1273	1125	ν_3-mode	SO_4^{2-}-dipole
1358/ 1466	1440	Stretching	-OH
1620	1638	ν_2-mode	H_2O-bending
3441/ 3480	3400	ν_3-mode	H_2O-stretcching

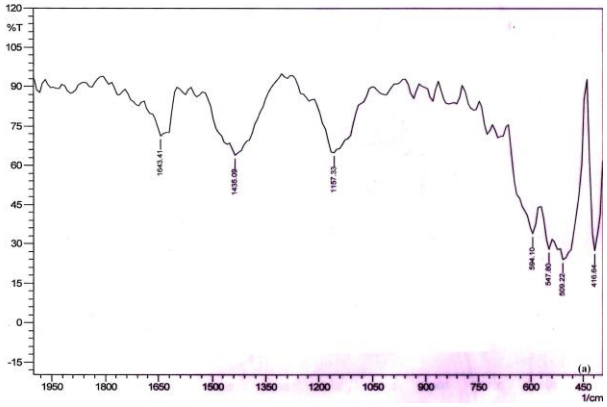

FIGURE 5.(a) FTIR transmission spectrum of as-prepared $Co_{0.5}Zn_{0.5}Fe_2O_4$ ferrite

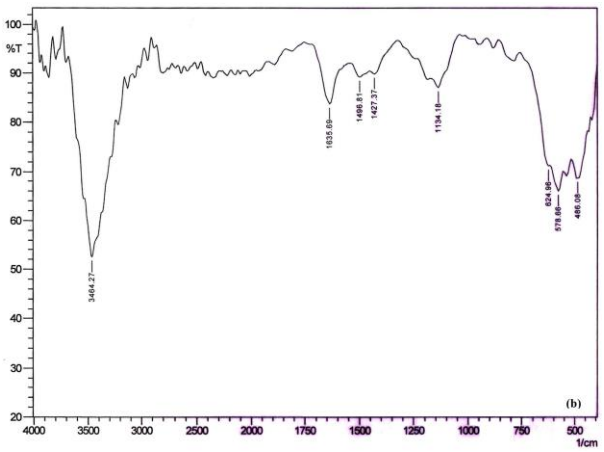

FIGURE 5.(b) FTIR transmission spectrum of as-prepared $Co_{0.2}Ni_{0.3}Zn_{0.5}Fe_2O_4$ ferrite

results was well confirmed by FTIR.

Electrical Properties

DC Resistivity

Fig. 6 shows the variation of dc electrical resistivity with increasing Nickel concentration in Co-Zn ferrites. It was found that dc resistivity is increased with the increasing content x of Nickel. It can be explained by Verwey's hopping mechanism. According to Verwey, the electronic conduction in ferrites is primarily because of hopping of electrons between ions of same element present in more than one valence state, distributed randomly over crystallographically equivalent lattice sites [14]. Most of the spinel type ferrites structurally form cubic close packed oxygen lattices with the cations at the octahedral (B) and the tetrahedral (A) sites. The distance between two metal ions at octahedral sites is smaller than the distance between a metal ion at an octahedral site and another metal ion at a tetrahedral site.

TABLE 3.(a) Wavenumbers and corresponding vibrational modes assignments of as-prepared ferrite for x = 0

Wavenumber (cm^{-1})		Mode assignment	Molecular Group
Observed	Standard		
417	450	ν_2-mode	Co^{2+}-Zn^{2+} in T_d-site
509/548 /594	550	ν_1-mode	Fe^{3+} in O_h-site
1157	1125	Stretching	-OH
1435	1440	Stretching	-OH
1643	1638	ν_2-mode	H_2O-bending

TABLE 3.(b) Wavenumbers and corresponding vibrational modes assignments of as-prepared ferrite for x = 0.3

Wavenumber (cm^{-1})		Mode assignment	Molecular Group
Observed	Standard		
486	450	ν_2-mode	Ni^{2+}-Co^{2+}-Zn^{2+} in T_d-site
579/625	550	ν_1-mode	Fe^{3+} in O_h-site
1134	1125	Stretching	-OH
1427/ 1497	1440	Stretching	-OH
1636	1638	ν_2-mode	H_2O-bending
3464	3400	ν_3-mode	H_2O-stretcching

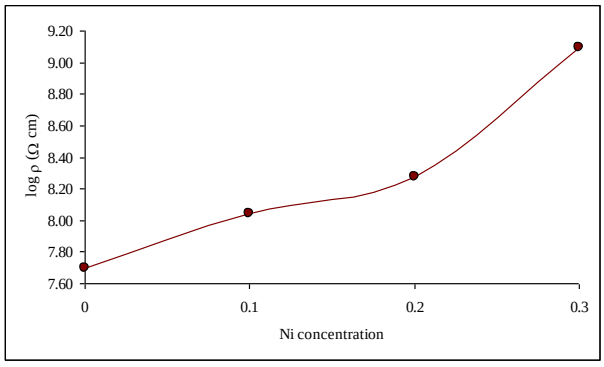

FIGURE 6. Variation of dc resistivity with different concentration of Nickel in $Co_{0.5-x}Ni_xZn_{0.5}Fe_2O_4$ ferrites

The electron hopping between octahedral and tetrahedral sites under normal conditions therefore has a very small probability compared with that for B–B hopping. Hopping between tetrahedral and tetrahedral sites does not exist for the simple reason that there are only Fe^{3+} ions at the tetrahedral sites and any Fe^{2+} ions formed during processing preferentially occupy octahedral sites only.

In addition, the hopping probability depends upon (a) the separation between the ions involved and (b) the activation energy. As Ni^{2+} ions strongly prefers to occupy A-sites [15], while Co^{2+} and Zn^{2+} ions partially occupy A-sites and B-sites. Thus, when Ni^{2+} ions increases at A-sites then some of the Fe-ions from B-sites will migrate towards the A-sites as a result the number of Fe^{2+} and Fe^{3+} ions at B-sites, which are responsible for electrical conduction in ferrites, will decrease.

This will limit the degree of conduction by blocking the Verwey's hopping mechanism resulting thereby an increase in resistivity. Further, the room temperature dc resistivity is of the order of ~10^8 Ωcm which make these nanoferrites suitable for microwave applications [16].

Temperature Dependent DC Electrical Conductivity Study

The temperature dependent dc conductivity of the $Co_{0.5-x}Ni_xZn_{0.5}Fe_2O_4$ ferrites obey an Arrhenius's expression,

$$\sigma = \sigma_0 \exp\left(\frac{-E_a}{kT}\right)$$

where, σ_0 is the pre-exponential factor, E_a is activation energy, k is Boltzmann's constant and T absolute temperature. Arrhenius's plot of the dc conductivity with reciprocal temperature is shown in Fig. 7. The graph shows that the increase in temperature leads to increase in conductivity, which is the normal behaviour of semiconducting materials and it obeys the well known Arrhenius relation [17]. The higher values of temperature for the samples help the trapped charges to be librated and participate in the conduction process which results increase in conductivity. According to the conduction mechanism in ferrites, the decrease in resistivity could also be related to the increase in the drift mobility of the thermally activated electrons.

The activation energies of the samples were calculated using the slope of Arrhenius's plot shown in Fig. 7 and the variation of activation energies with Nickel concentration is shown in Fig. 8. It was found that the activation energy is decreased with increasing Ni concentration of x = 0 – 0.2 in $Co_{0.5-x}Ni_xZn_{0.5}Fe_2O_4$ ferrites and slightly increased at x = 0.3. In general, for the ferrite samples, the activation energy is often associated with the variation of mobility of charge carriers rather than with their concentration. The charge carriers are considered as residing at the vacant sites and conduction occurs via a hopping process which depends upon the activation energy [13]. Due to

addition of Ni inter ionic distance increase which enhances the barrier height encountered by the charge carriers during the hopping process and consequently, it enhances the activation energy.

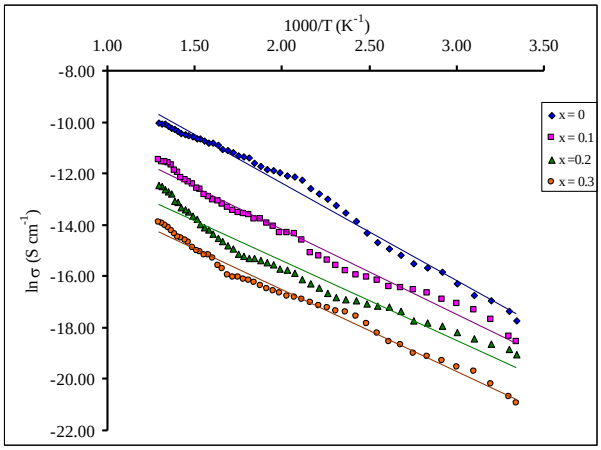

FIGURE 7. Arrhenius's plot of the dc conductivity with reciprocal temperature of $Co_{0.5-x}Ni_xZn_{0.5}Fe_2O_4$ ferrites

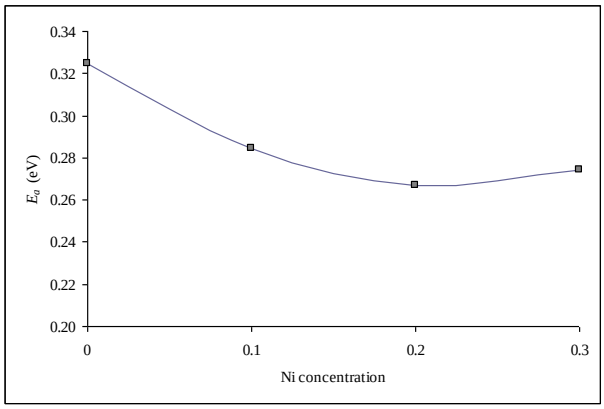

FIGURE 8. Variation of activation energies with Nickel concentration in $Co_{0.5-x}Ni_xZn_{0.5}Fe_2O_4$ ferrites

CONCLUSION

Nanosized $Co_{0.5-x}Ni_xZn_{0.5}Fe_2O_4$ ferrites were successfully prepared by co-precipitation method. The XRD studies reveal that nanosized of spinel ferrites formed by chemical co-precipitation method were cubic crystalline materials. The obtained lattice parameters were well discussed. Phase formation of the samples was confirmed by FTIR spectroscopy using the appearance of the spectral lines. DC electrical resistivity was increased with increasing contents x of Ni and it can be explained using Verwey's hopping mechanism. The temperature dependent dc conductivity and activation energy were studied and discussed. The increase in dc resistivity with increasing Ni concentration in Co-Zn ferrite suggests that the samples can be used as microwave devices.

ACKNOWLEDGEMENT

The authors feel indebted to Dr. Zaya Oo, Senior Lecturer, School of Engineering and Science, Curtin University of Technology, Sarawak, Malaysia, for his stimulating suggestions.

REFERENCES

1. V. G. Harris and C. Vittoria, *J. Magn. Magn. Mater*, **321**, January (2009), pp. 2035-2047.
2. R. Iyer, R. Desai and R. V. Upadhyay, *Bulletins Materials Science*, **32**, April (2009), pp. 141-147.
3. I. Ahmad and M. T. Farid, *J. World Appl. Sci*, **19**, April (2012), pp. 464-469.
4. G. Sathishkumar, C. Venkataraju, K. Sivakumar *Mate. Sci. Appl*, **1**, (2010), pp. 19-24.
5. K. H. Maria1, S. Choudhury and M. A. Hakim, *Int. Nano Lett*, **3**, (2013), pp. 1-10.
6. P. D. Thang, G. Rijnders and D. H. A. Blank, *J. Magn. Magn. Mater*, **295**, (2005), pp. 251-256.
7. M. U. Islam, M. U. Rana and Abbas, *Mater. Chem. Phys*, **57**, (1998), pp. 190-193.
8. R. K. Sharma and P. A. Joy, *Mater. Lett*, **59**, (2005), pp. 3402-3405.
9. S. J. Singh, S. K. Barthwal and K. Chandra, *J. Solid State Chem*, **178**, (2005), pp. 3183-3189.
10. I. H. Gul and A. Maqsood, *J. Magn. Magn. Mater*, **311**, (2007), pp. 494-499.
11. K. Praveena, K. Sadhana and S. R. Murthy, *Int. J. Sci. Res. Publ*, **3**, (2013), pp. 1-4.
12. M. Thomas and K. C. George, *Indian J. Pure Appl. Phys*, **47**, (2009), pp. 81-85.
13. N. Kasapoglu and H. Bayrakdar, *Turkey J. Chem*, **31**, (2007), pp. 659-976.
14. A. Lakshman, P. S. V. S. Rao, B. P. Rao and K. H. Rao, *J. Phys D: Appl. Phys*, **38**, February (2005), pp. 673-678.
15. A. Z. Fawzi, A. D. Sheikh and V. L. Mathe, *J. Alloys and Compounds*, **502**, July (2010), pp. 231-235.
16. R. Rani, G. Kumar, K. M. Batoo and M. Singh, *Am. J. Nanomater*, **1**, (2013), pp. 9-12.
17. S. N. Patil and B. P. Ladgaonkar, *Int. J. Adv. Res. Electr, Electron. Instrum. Engin*, **19**, August (2013), pp. 3813-3819.